

A morphometric assessment and classification of coral reef spur and groove morphology



S. Duce ^{a,*}, A. Vila-Concejo ^a, S.M. Hamylton ^b, J.M. Webster ^a, E. Bruce ^a, R.J. Beaman ^c

^a Geocoastal Research Group, School of Geosciences, University of Sydney, Sydney, New South Wales 2006, Australia

^b School of Earth and Environmental Sciences, University of Wollongong, Wollongong, New South Wales 2522, Australia

^c College of Science, Technology and Engineering, James Cook University, Cairns, Queensland 4870, Australia

ARTICLE INFO

Article history:

Received 18 January 2016

Received in revised form 23 April 2016

Accepted 25 April 2016

Available online 27 April 2016

Keywords:

Coral reef geomorphology

Spur and groove

Ecomorphodynamics

Morphometrics

Reef evolution

ABSTRACT

Spurs and grooves (SaGs) are a common and important feature of coral reef fore slopes worldwide. However, they are difficult to access and hence their morphodynamics and formation are poorly understood. We use remote sensing, with extensive ground truthing, to measure SaG morphometrics and environmental factors at 11,430 grooves across 17 reefs in the southern Great Barrier Reef, Australia. We revealed strong positive correlations between groove length, orientation and wave exposure with longer, more closely-spaced grooves oriented easterly reflecting the dominant swell regime. Wave exposure was found to be the most important factor controlling SaG distribution and morphology. Gradient of the upper reef slope was also an important limiting factor, with SaGs less likely to develop in steeply sloping ($>5^\circ$) areas. We used a subset of the morphometric data (11 reefs) to statistically define four classes of SaG. This classification scheme was tested on the remaining six reefs. SaGs in the four classes differ in morphology, groove substrate and coral cover. These differences provide insights into SaG formation mechanisms with implications to reef platform growth and evolution. We hypothesize SaG formation is dominated by coral growth processes at two classes and erosion processes at one class. A fourth class may represent relic features formed earlier in the Holocene transgression. The classes are comparable with SaGs elsewhere, suggesting the classification could be applied globally with the addition of new classes if necessary. While further research is required, we show remotely sensed SaG morphometrics can provide useful insights into reef platform evolution.

© 2016 Elsevier B.V. All rights reserved.

1. Introduction

Spurs and grooves (SaGs) are distinctive features of fore reef slopes worldwide. Spurs are parallel ridges of carbonate material (coral and algae) separated by regularly spaced channels (grooves) forming a characteristic “comb-tooth” pattern (Gischler, 2010). SaG systems have been documented in every global reef province (e.g. Weydert, 1979; Sheppard, 1981; Shinn et al., 1981; Kan et al., 1997a; Rogers et al., 2015). They represent one of the most biodiverse and productive zones of modern reefs (Perry et al., 2013) and are believed to act as natural breakwaters (Munk and Sargent, 1954), regulating the hydrodynamic energy and nutrients received by reef platforms and thus affecting reef biogeography (Odum and Odum, 1955). Despite their importance, the geomorphology, formation processes and ecomorphodynamics of SaG systems are poorly understood (Gischler, 2010; Rogers et al., 2013) particularly in the Great Barrier Reef (GBR), Australia (Duce et al., 2014). Their underrepresentation in the literature is likely due to the difficulties of working in these high-energy environments (Guilcher, 1988).

There is considerable debate as to whether the formation of SaGs is driven by predominantly erosional or constructional processes, or by a combination of both (Sneh and Friedman, 1980; Guilcher, 1988; Storlazzi et al., 2003; Gischler, 2010). Erosional processes include wave and current driven abrasion of grooves by rubble and/or sediment (Cloud, 1954); “pruning” of corals on spurs and spur walls by occasional hurricanes (Blanchon and Jones, 1997); and limestone solution of antecedent topography by fresh water flows during sea level low-stands to form grooves (Newell, 1954; Purdy, 1974). Constructional processes include water motion promoting aligned coral growth and eventual colony coalescence to form spurs (Shinn, 1963; Shinn et al., 1981; Kan et al., 1997a); and coral debris being washed together and rapidly cemented by robust, wave-resistant coralline algae forming spurs (Storlazzi et al., 2003; Blanchon, 2011; Littler and Littler, 2011). Which process dominates is thought to be a function of environmental factors (primarily wave energy) (Storlazzi et al., 2003; Shinn, 2011) and the rate of Holocene sea-level change (Gischler, 2010).

The morphology of SaG systems varies markedly both between and within reefs (Duce et al., 2014). However, comparison between the features globally is difficult as there is no standard definition of morphometric parameters and authors report different metrics. For example, Roberts et al. (1977) and Storlazzi et al. (2003) report “wavelengths”

* Corresponding author.

E-mail address: stephanie.duce@sydney.edu.au (S. Duce).

(i.e. distance between consecutive spur crests) and “amplitude” (i.e. the distance from spur crest to groove trough) while [Roberts \(1974\)](#) and [Blanchon and Jones \(1997\)](#) report “spur frequency” (i.e. number of spurs per 1000 m of reef) and; [Munk and Sargent \(1954\)](#) report the “width and spacing” of grooves. In addition, descriptions are frequently qualitative and adjective-based rather than quantitative ([Duce and Janowicz, 2010](#)). For example, adjectives such as “narrow” are used in place of quantitative values to describe groove width ([Roberts, 1974](#); [Blanchon and Jones, 1997](#); [Hamanaka et al., 2015](#)).

Understanding SaGs globally is further complicated by differing terminology. A comprehensive review of reef terminology within published literature identified 12 different terms used to refer to SaGs ([Kuchler, 1986a](#)). In fact, [Stoddart \(1978\)](#) suggested that much of the controversy surrounding “the nature” and formation of SaGs arose from the term being applied too broadly to a variety of features which differed in morphology and origin.

Meaningful classification and clear definition is critical to effective management of natural systems ([Elliott and McLusky, 2002](#); [Duce, 2009](#)). The classification of geomorphic features is also an important step in understanding their formation, evolution and interactions with the environment. Two approaches to classification have been adopted by geomorphologists: those based on form and, those based on processes ([Drăguț and Blaschke, 2006](#)). Several publications have described different types of SaGs based on observations of both form and processes. These SaG types and the formation processes suggested in the literature are summarized in [Table 1](#).

As evidenced in [Table 1](#) there are different types of SaGs, likely dominated by different formation processes, with different implications to reef ecology and reef platform evolution. Identifying and clearly defining these SaG types is important to understand and manage coral reefs into the future. Ideally this requires extensive hydrodynamic data and dating of sub-surface material from many sites. However, such data are extremely difficult and costly to collect from this dynamic

Table 1
Types of spurs and grooves and their suggested formation mechanisms from the published literature.

Location (source)	Types and description	Data used	Suggested formation mechanisms
Caribbean, western Indian Ocean, French Polynesia (Gischler, 2010)	Indo-Pacific <i>Dimensions:</i> wide flat spurs. Narrow V-shaped grooves <i>Groove floor:</i> sparse sand and rubble <i>Spur cover:</i> coralline algae and few corals Atlantic <i>Dimensions:</i> U-shaped <i>Groove floor:</i> abundant sand <i>Spur cover:</i> high coral cover	Qualitative observations and literature review	Indo-Pacific - Erosion dominated Atlantic - largely constructive. Driven by differences in Holocene sea-level change (transgressive-regressive in the Indo-Pacific and transgressive in the western Atlantic)
Molokai, Hawaii (Storlazzi et al., 2003)	Higher energy spur and groove <i>Depth:</i> 5–10 m <i>Dimensions:</i> mean spur height 0.5 m, ~87 m between spur crests <i>Spur cover:</i> lower total coral cover Lower energy spur and groove <i>Depth:</i> 15–20 m <i>Dimensions:</i> mean spur height 1.1 m, ~93 m between spur crests <i>Spur cover:</i> higher total coral cover	Quantitative bathymetric data and wave modelling	Waves are the primary control, light and antecedent topography plays a lesser role. Higher energy spurs constructed primarily by cementation of coral rubble. Lower energy spurs dominated by in situ coral growth.
Caribbean, Indo-Pacific (Blanchon and Jones, 1997 ; Blanchon, 2011)	Shallow spur and groove (2 types) <i>Depth:</i> to 15 m <i>Dimensions:</i> One spur every 6–10 m. Spurs 4–8 m wide, 2–8 m high with steep to overhanging sides. Grooves 1–3 m wide <i>Groove floor:</i> coral gravel <i>Spur cover:</i> <ol style="list-style-type: none"> 1. Coralline algae dominated 2. Coral dominated Chute and buttress <i>Depth:</i> ~25–60 m <i>Dimensions:</i> Buttresses ~100 m long, 10 m wide, tapering shoreward. One buttress every 30 m or more	Literature review, bathymetric data, short-cores and observations	Distribution and form controlled by wave energy. Buttresses and coral dominated spurs constructional and grow towards the reef shelf with “pruning” by storms. Coralline algae dominated spurs are similar but may (the age structure of these spurs remains unknown) grow seaward.
Grand Cayman Island (Caribbean) (Roberts et al., 1975 ; Roberts et al., 1977)	Wave dominated spur and groove <i>Depth:</i> to 8 m <i>Dimensions:</i> ~43 m between grooves <i>Groove floor:</i> little sediment <i>Spur cover:</i> moderate coral cover Current dominated spur and groove <i>Depth:</i> 8–22 m <i>Dimensions:</i> ~50 m between grooves <i>Groove floor:</i> extensive sediment <i>Spur cover:</i> abundant coral cover	Bathymetry, wave and current measurements	Associated with eustatic sea-level history. Current dominated SaGs initiated early in Holocene sea-level rise and have had longer to mature and continued to grow under less wave stress as water deepened.
French Polynesia (Battistini et al., 1975)	Furrowed platform <i>Dimensions:</i> ~30–40 m long Buttresses and valleys <i>Depth:</i> ~12 m <i>Dimensions:</i> ~60 m long <i>Groove floor:</i> bare or covered in reef detritus Outer slope spur and grooves <i>Depth:</i> ~12–27 m <i>Dimensions:</i> ~100 m long <i>Groove floor:</i> bare or covered in reef detritus	Qualitative observations	Furrows “cut in the direction of the slope”.

and potentially hazardous zone. We propose that SaG morphometrics, measurable using remote sensing techniques, can be used to identify different types of SaGs and provide insight into their formation.

The purpose of this research is to assess relationships between SaG morphometrics and environmental factors; identify and define different classes of SaGs; and evaluate the implications of the classification to understanding SaG formation. This research presents a novel, statistical approach to achieve these aims using remotely sensed data. In total, 11,430 grooves were analyzed at 17 reefs in the Capricorn-Bunker Group, southern GBR, Australia. A subset of the data (11 reefs for which high resolution bathymetric data were available) were used to develop a statistically significant classification scheme. This scheme was then formally defined and applied to all 17 study reefs. This study region was chosen as it represents a diversity of reef platforms allowing relevant global comparison. The geology and ecology of the region is well studied (Hopley et al., 2007) and remotely sensed imagery and bathymetric data in the area were available at high resolution (Beaman, 2010).

2. Regional setting

The Capricorn-Bunker Group (CBG) comprises the southern-most 22 reefs and 15 reef islands in the Great Barrier Reef Marine Park extending from North Reef No. 1 (23.18°S 151.9°E) 135 km south to Lady Elliot Island (24.11°S 152.7°E) (Fig. 1). The group is situated 80 km offshore from the port city of Gladstone, Queensland (Australia) between the Curtis and Capricorn channels. Inter-reef depths range from 35 to 60 m (Jell and Webb, 2012) and the area is composed exclusively of carbonate sediment (Mathews et al., 2007).

Seventeen CBG reefs were examined in this study. The reefs vary considerably in size (reef flat areas from 1 to 29 km^2), shape, and exposure to wave energy (Fig. 1). Seven reefs are classified as lagoonal (mature) and ten as planar (senile) under the Hopley (1982) morphogenetic classification (Table 2). The reefs are composed of thickness between 9 and 20 m of Holocene reef facies growing on top of a Pleistocene reef basement (Jell and Webb, 2012; Dechnik et al., 2015). The timing of Holocene reef initiation in the CBG is between 7.6 and 8.3 thousand years ago (ka) (Dechnik et al., 2015). Recent dating suggests the windward margin of One Tree Reef reached mean sea level (MSL) around 6.3 ka (Dechnik et al., 2016) while the leeward margin of Heron Reef reached MSL between 6 and 7 ka (Webb et al., 2016). Most spurs and grooves occur across the upper reef slope, the subtidal portion of the reef mass immediately seaward of the reef crest (the outer-most part of the reef flat) down to a noticeable break in slope and/or change in substrate (Kuchler, 1986b) (Fig. 3). The upper reef slope extends to a depth of approximately 15 m beyond which reef growth continues down the lower reef slope to about 30–35 m where it merges with the surrounding seafloor. Several reefs are connected by a terrace at approximately 15 m depth (e.g. North West, Broomfield and Wilson; and Heron and Sykes further south) (Fig. 1). The region is dominated by southeasterly trade winds, with average speeds of 20 to 40 km h^{-1} for approximately 70% of the year (Jell and Webb, 2012). The wave climate of the region is characterized by deep water swell driven by storms and trade winds (Hopley et al., 2007). The global hind cast wave model, NOAA WAVEWATCH III®, shows average significant wave heights of 1.15 m, from a predominantly east-southeasterly direction (Harris and Vila-Concejo, 2013). Given the location of the CBG, 80 km offshore from the mainland and only 10 to 20 km west of the continental shelf edge, the majority of the studied reefs are exposed to unimpeded oceanic swells (Fig. 1). Six of the studied reefs (Tryon, North West, Polmaise, Masthead, Wistari and Heron) receive some protection from the eastern-most study reefs. The CBG region is meso-tidal with a tidal range of 2.0–3.3 m and strong tidal currents can occur (Jell and Webb, 2012). The area is also exposed to occasional cyclones (Woolsey et al., 2012).

3. Methods

In classifying different types of reef features, Andrefouet (2011) stated that reef geomorphology, geometrics and hydrodynamics should be taken into account. To meet this aim, and also define a classification which could be broadly applied to SaG systems worldwide, this study employed the following seven criteria:

1. Classes must be based on variables obtainable from remotely sensed data;
2. Definitions should be as simple as possible to be easily applied elsewhere;
3. Membership to each class should be exclusive (i.e. each groove can only qualify for one class);
4. Differences between classes are maximized (statistically significant difference between each class);
5. Variability within class is minimized;
6. Classes reflect the spatial structure/distribution of the data; and
7. Classes reflect physical characteristics observed.

Fig. 2 shows an overview of the methodology employed. First, SaG morphometrics and environmental factors were calculated. Considerable ground truthing was also conducted. Exploratory spatial data analysis (Anselin et al., 2006) was then used to understand the structure and trends in the data and assess the relationships between SaG morphometrics and environmental factors. Initial classification of SaGs was performed on SaGs from 11 reefs ($n = 7486$) to identify four morphometrically distinct classes of SaG. The classification was then formally defined in SQL and applied to the six remaining reefs ($n = 3944$). Classification performance was evaluated statistically and with ground truth data. The implications of the classification for understanding SaG formation was assessed through comparison to SaGs at other sites in the published literature.

3.1. Calculate SaG morphometrics

3.1.1. Image analysis and digitizing

Remotely sensed imagery was examined and SaG zones were identified around each reef (Table 2). Grooves were the most visible feature as their light colored floor is distinct against the darker, reef material of spurs. As discussed in Duce et al. (2014), the features were often too small (~1 m), cryptic, and at times, spectrally similar to other features for the use of automatic image classification techniques. Thus, ArcGIS 10.1 was used to visually assess imagery and manually digitize grooves at a scale of 1:1000. Where Google My Maps imagery was of sufficiently high spatial resolution, this free online mapping tool was used to digitize grooves for export to ArcGIS. The main limitations of this method were the presence of sun-glint and breaking waves, and the optical water depth limits (Duce et al., 2014). Given reefs in the CBG do not extend much below ~35 m, at which depth the inter-reefal continental shelf dominated by soft sediment occurs (Mathews et al., 2007), it is unlikely that any significant grooves were missed due to the depth limitations of the imagery. Ground truthing via SCUBA to 30 m off the southern slope of One Tree Reef did not identify any additional SaG features.

3.1.2. Morphometric parameters

Six quantitative morphometrics were measured at each groove (groove length, orientation, sinuosity and spacing at the start of the zone and at the -3 and -10 m depth contours). ArcGIS 10.1 was used to quantify these metrics.

Groove length was calculated as the path distance along the groove in meters. To calculate the orientation of each groove, in degrees, a straight line was created from groove start point (reef-ward side) to end point (seaward side) and the azimuth of this line was obtained. Given that orientation values are measured on a circular scale, on which 0° and 360° are almost identical but the values are numerically

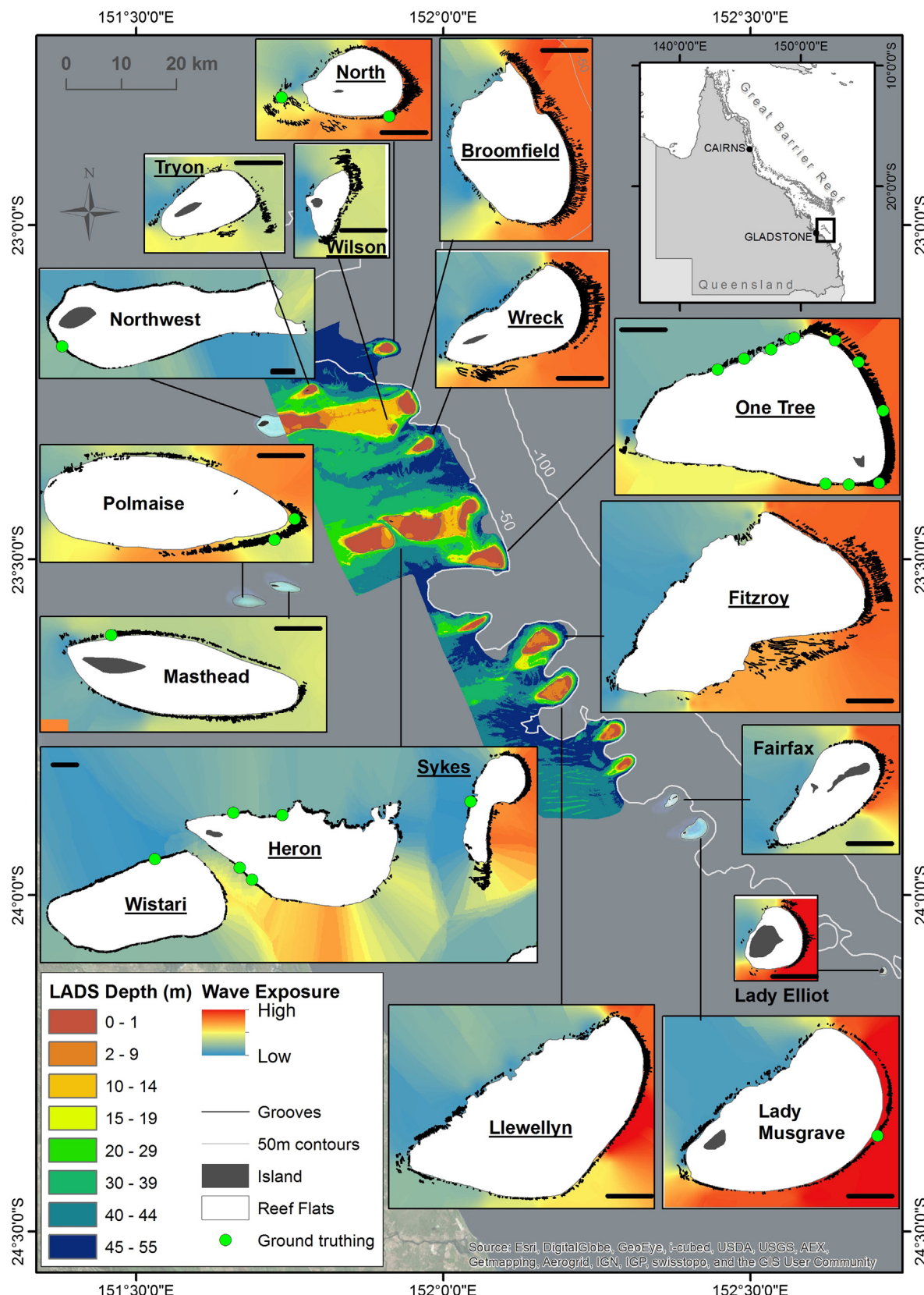


Fig. 1. Map showing the study site in the Capricorn-Bunker Group of the southern Great Barrier Reef (overview inset on top right) with high resolution Laser Airborne Depth Sounder (LADS) bathymetry. The 17 reefs included in this study, overlaid on the relative wave exposure surfaces, are shown with black scale bars denoting 1 km. The digitized grooves are mapped in black. Ground truth sites are marked with dots. Reefs with LADS data, used to develop the classification, are underlined.

Table 2

Summary of image sensor, bathymetric data source and ground truthing at each study reef. Reefs are listed from north to south along with morphogenetic reef class (Hopley, 1982) and presence of cays. WorldView-2 satellite imagery is abbreviated to "WV-2". Bathymetry acquired using a Laser Airborne Depth Sounder is abbreviated to "LADS", while "gbr100" bathymetry refers to digital bathymetric data compiled from a range of sources. The spatial resolution of bathymetric data is given in parenthesis. Asterisks denote the 11 reefs used to develop the classification. The remaining six reefs were used to validate the classification.

Reef	Reef class	Imagery	Bathymetry	Ground truthing
North*	Planar (cay)	WV-2	LADS (25 m)	Video surveys western and southeastern sides
Tryon*	Planar (cay)	Google My Maps	LADS (25 m)	–
Broomfield*	Lagoonal	WV-2	LADS (25 m)	–
Wilson*	Planar (cay)	WV-2	LADS (25 m)	–
North West	Planar (cay)	Google My Maps WV-2	gbr100 (100 m)	Photo transect southwestern side
Wreck*	Planar (cay)	WV-2	LADS (25 m)	–
		Aerial Photo		
Sykes*	Planar	Google My Maps WV-2	LADS (25 m)	Photo transect on western side
Heron*	Lagoonal (cay)	WV-2	LADS (25 m)	Photo transects at 2 northern sites and 2 southwestern sites
		Quickbird		
Wistari*	Lagoonal	Google My Maps WV-2	LADS (25 m)	Photo transect on the northwestern side
Masthead	Planar (cay)	GeoEye	gbr100 (100 m)	Video surveys on northwestern side
Polmaise	Planar	WV-2	gbr100 (100 m)	Photo transects on eastern and southeastern sides
One Tree*	Lagoonal (cay)	WV-2	LADS (25 m)	Photo transects at 11 sites around the northern, eastern and southern sides
		Aerial Photo		
Fitzroy*	Lagoonal	Google My Maps	LADS (25 m)	–
Llewellyn*	Lagoonal	WV-2	LADS (25 m)	–
Fairfax	Planar (2 cays)	Aerial Photo	gbr100 (100 m)	–
Lady Musgrave	Lagoonal (cay)	GeoEye	gbr100 (100 m)	Photo transect on southeast side
Lady Elliot	Planar (cay)	Google My Maps	gbr100 (100 m)	–

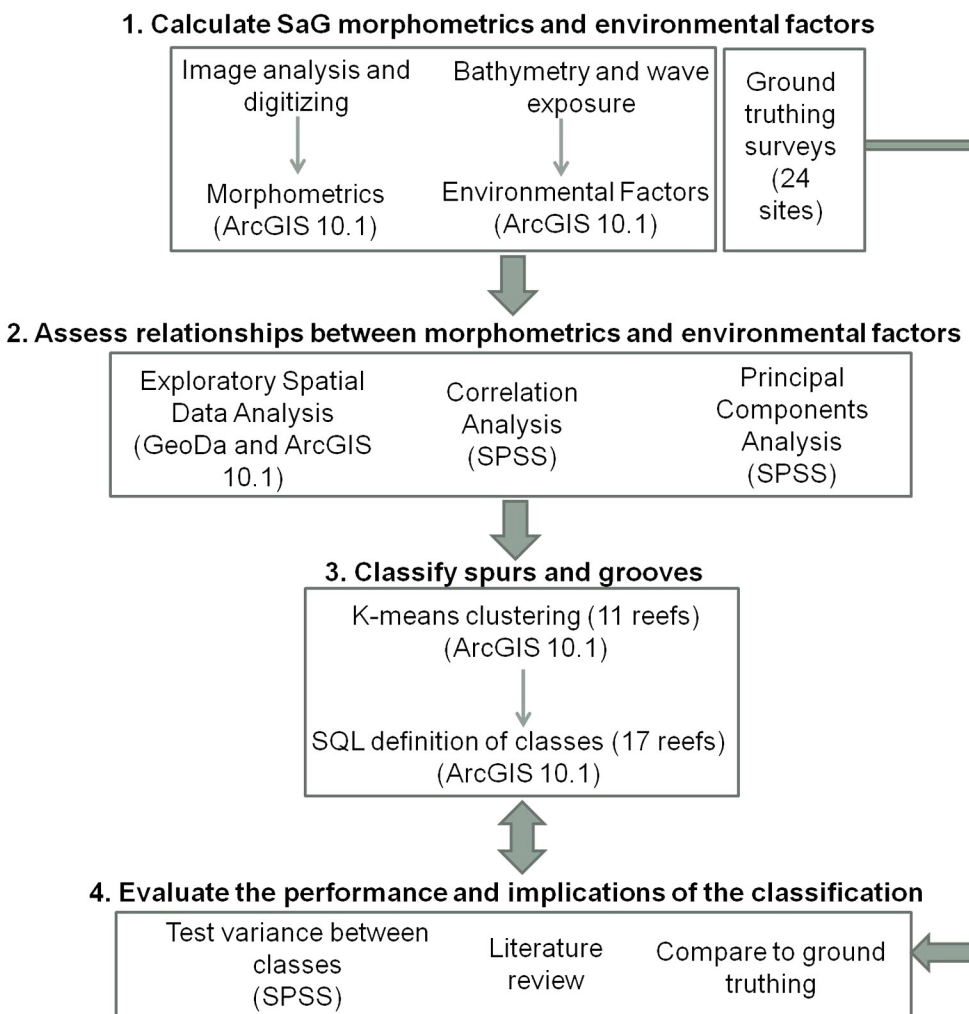


Fig. 2. Overview of methodology employed. Software programs used at each step are in parenthesis.

different, traditional statistics cannot be performed (Zar, 1999). Thus, the orientation of each groove was first converted from degrees to radians, then trigonometric functions cosine and sine were applied to calculate 'northness' and 'eastness' values using the following equations

derived from Wallace and Gass (2008):

$$N = \cos(x) \quad (1)$$

$$E = \sin(x) \quad (2)$$

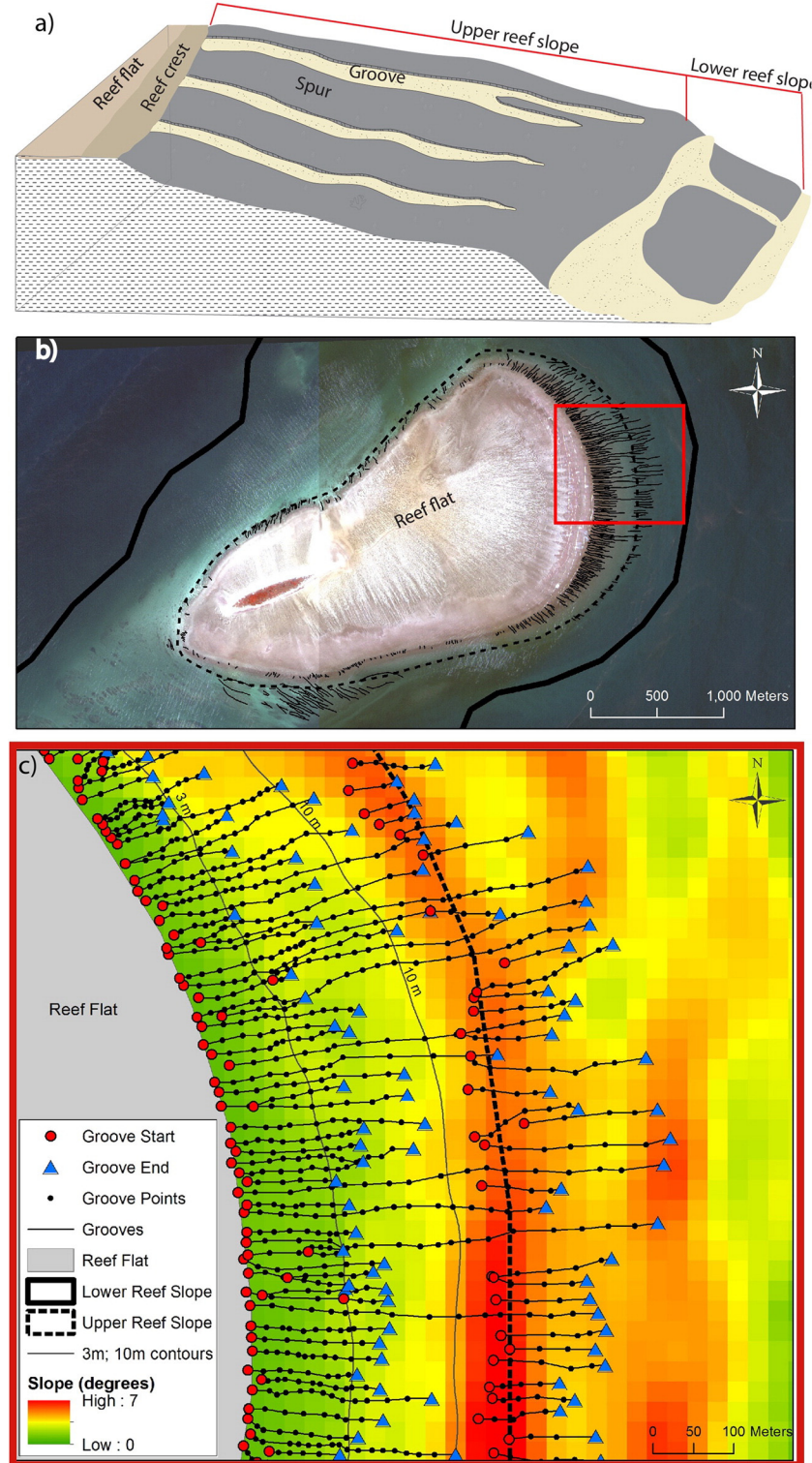


Fig. 3. An overview of spurs and grooves showing: a) A schematic diagram depicting the geomorphic zones discussed. Spurs and grooves, including a bifurcating groove, are presented. b) An overview of Wreck Reef showing digitized grooves and the boundaries of the upper (dotted black line) and lower reef slope (bold line). The square inset shows the area of (c). c) A map showing digitized groove lines with a series of points across which environmental variables were averaged for each groove. Slope of the reef front is shown in degrees with the upper reef slope delineated (black dashed line) along the clear break in slope (dark, steep area). Start and end points of grooves are depicted by circles and triangles respectively. The distance between each groove (spacing) was measured at the start of the zone and where each groove intersects the –3 and –10 m contours (grey lines).

where x is the clockwise angle from north of each groove. Northness (N) values range from 1 for a northerly orientation (i.e. 0°), to -1 for a southerly orientation (i.e. 180°). Eastness (E) values range from 1 for an easterly orientation (i.e. 90°), to -1 for a westerly orientation (i.e. 270°).

Sinuosity, extent to which each groove deviates from a perfectly straight line; S , was calculated using the ratio:

$$S = D/L \quad (3)$$

where D is the straight-line distance covered and L is the measured length of the path (i.e. groove) (Benhamou, 2004). Sinuosity takes positive values equal to or < 1 , where 1 indicates a perfectly straight groove.

The spacing between consecutive grooves was calculated at the start of the SaG zone, usually where the grooves meet the reef crest, and at the -3 and -10 m contours. If grooves were >250 m apart they were not included in the calculation of mean spacing as they were deemed to be part of a different set. Note was also taken of the context of each groove within the reef slope. The locations of initiation and termination of each groove were recorded as binary variables (yes/no) for the following questions: Does the groove start at the reef crest? Does the groove finish within the upper reef slope (or open out onto the lower reef slope or surrounding seafloor)?

3.1.3. Ground truth surveys

Spurs and grooves were visited at 24 sites across nine reefs between October 2013 and May 2015 (Table 2 and Fig. 1). Georeferenced underwater photo transects were conducted via snorkel or SCUBA using a digital underwater camera and continuously logging Global Positioning System (GPS) attached to a float directly above the photographer (Roelfsema and Phinn, 2010). Georeferenced video surveys were performed by lowering an underwater video camera from a boat to the sea floor and recording ~ 30 s of footage and recording the location using GPS (Hamilton et al., 2013). Observations were made of the following six variables:

1. Width of spurs in meters;
2. Width of grooves in meters;
3. Height of spurs from the spur crest to the bottom of the adjacent groove;
4. Substrate of groove;
5. Dominant coral morphology and percent cover; and
6. Morphology of spur walls (i.e. vertical, overhanging, or gently sloping).

3.1.4. Calculation of environmental factors

A bathymetric grid with a resolution of 25 m, developed from Laser Airborne Depth Sounder (LADS) data, was used for 11 of the 17 reefs (Table 2). For the remaining six reefs lacking LADS data, a bathymetry grid, "gbr100", with a resolution of ~ 100 m was used (Beaman, 2010). Both grids referred to the WGS84 horizontal datum and mean sea level (MSL) vertical datum. Slope and aspect were calculated as continuous surfaces. Neither bathymetric layer was of high enough resolution to resolve SaG topography. Nevertheless the data provided insight into the broad reef topography in which the SaG zone occurs. Each groove line was converted to a series of points at the vertices (Fig. 3). Depth (m), slope (degrees) and aspect (degrees) were recorded at each point. Mean, minimum and maximum depth, depth range, mean and maximum slope, and mean aspect were then calculated for each groove from these points. The bathymetry data and remotely sensed imagery were used to define the upper reef slope (Fig. 3). The width of this zone was measured at 500 m intervals around each reef rim and interpolated to create a continuous surface representing width. The average width of the upper reef slope at each groove was calculated.

Wave exposure is a key variable controlling coral reef communities and geomorphology (Harborne et al., 2006). As explained by Ekebom

et al. (2003), fetch distance (the distance that wind can blow across a water body without being interrupted i.e. by reef or land) can be combined with typical wind speed and direction data to estimate theoretical wave exposure. A GIS-based model (GREMO) (Pepper and Puotinen, 2009) was used to create a continuous, spatially explicit grid of relative wave exposure around each reef. GREMO normalizes wave exposure values to a theoretical maximum to return a dimensionless exposure value that can be compared between reefs. We calculated fetch distance in 30° increments every 250 m around each reef. Wind speed and direction statistics were calculated from the Bureau of Meteorology weather stations at Heron Island or One Tree Island. The relative exposure values were interpolated to create a continuous wave exposure surface around each reef (Fig. 1). The mean relative wave exposure value at each groove was then calculated. For presentation in Table 3, the relative wave exposure values were split into three equal-interval classes: High (the top 1/3 of values), Medium and Low (the bottom 1/3 of values). This method does not take into account depth induced wave refraction and other hydrodynamic processes, and thus only provides a proxy for relative wave energy (Duce et al., 2014).

3.2. Assess relationships between morphology and environmental parameters

Extensive exploratory spatial data analysis was conducted in ArcGIS 10.1 and the spatial statistics package GeoDa 1.4.1 (Anselin et al., 2006), and additional statistical analyses were performed in SPSS 22.0. Descriptive statistics were calculated for each variable and data distributions were examined. Spatial autocorrelation was assessed for each variable using Univariate Local Moran's I tests (Anselin, 1995) with spatial weighting based on eight K-nearest neighbors. A Spearman's rank-order correlation was performed to investigate individual relationships between environmental and morphometric variables. This correlation method was chosen as data were not normally distributed and contained outliers which could not be disregarded (Schuenemeyer and Drew, 2001). A Principal Component Analysis (PCA) was performed to further examine data structure and explore more complex relationships between variables. This technique simplifies the dataset to a series of uncorrelated orthogonal components representing the entire variance of the dataset (Demesar et al., 2013; Kain et al., 2015). The PCA was performed on a scale-independent correlation matrix.

3.3. Classify SaGs

Cluster analysis was conducted in ArcGIS 10.1 to explore meaningful ways in which spurs and grooves could be grouped into classes. A K-means clustering algorithm that groups features into a user specified number of classes based on their attributes was employed (Jain, 2010). This clustering method was chosen for its computational efficiency, which was critical given the large sample size, and the ability for the output clusters to be viewed on a map (Jain, 2010). The K-means clustering analysis was performed without spatial constraint on the 11 reefs ($n = 7486$) for which high-resolution LADS bathymetric data were available. Different combinations of attributes (morphometric variables) and numbers of classes were trialed iteratively to determine an optimal combination. The output parallel box plots are presented in Supplementary Fig. S1. A ratio representing within-group similarity and between-group differences, the Calinski-Harabasz pseudo F-statistic (Calinski and Harabasz, 1974), indicated the optimal number of groups for this dataset to be four. K-means clustering defines classes in a way that maximizes variability between classes (classification criterion #4, Section 3, paragraph 1) and minimizes variability within classes (classification criterion #5). However, the classes created are complex and do not have exclusive membership (not meeting classification criteria #2 and #3). Thus, once the optimal K-means clustering solution had been reached, it was translated into structured query

language (SQL) definitions for each of the four classes. These SQL definitions were applied across the additional six reefs ($n = 3944$).

3.4. Evaluate the performance and implications of the classification

Statistical tests and qualitative evaluation of ground truthed images were undertaken to evaluate the classification. Kruskal-Wallis H tests were performed to judge whether differences between classes were statistically significant (classification criterion #4). The distributions of data within each variable were assessed for each group using box plots to ensure that variability within groups was minimal and that between groups was maximal (classification criteria #4 and #5). Ground truth data (Section 3.1.3) were examined to determine if the classes accurately reflected the physical characteristics of the systems (classification criterion #7). Two sites were field surveyed from Class 1, six from Class 2, six from Class 3 and ten from Class 4 (Table 2, Fig. 3).

4. Results

4.1. SaG morphometrics

There is no clear relationship between reef flat size and the number of SaGs with North West (the largest of the reefs by area) having the least grooves (173) (Table 3). There are 154 grooves per square kilometer of reef flat on average throughout the CBG but this varies from 6 km^{-2} at North West to 1077 km^{-2} at Wilson (Table 3). The majority (65%) of grooves across the CBG extend from the reef crest down the upper reef slope. The remaining 35% of grooves are not connected to the reef crest and either start further down the upper reef slope or are located on an adjacent reef terrace (e.g. North, Tryon, Sykes and Fitzroy). The SaG zone at most reefs ranged in depth from approximately 0 to 19 m, with a mean depth of 5 m (Table 3). The maximum depth at which a groove was measured was –31 m (Wreck).

Groove length throughout the CBG ranges from a minimum of 1.5 m (Fairfax) to a maximum of 654 m (Sykes) with a median length of 31 m, a mean of 52 m, and high variability both between and within reefs with mean standard deviation (SD) of 53 m (Table 3). Mean exposure values vary between reefs from 0.17 at Wilson to 1.19 at Lady Elliot (Table 3). As shown in Fig. 1, each reef is characterized by a windward, exposed (eastern) side and a leeward, protected (western) side creating considerable within-reef variability in exposure values. The SD value in groove length is greatest at reefs with “High” exposure (67 m on average) and smallest at reefs with “Low” exposure (26 m) (Table 3). Groove length shows spatial autocorrelation (Moran's $I = 0.66$) with the longest grooves occurring on the eastern sides of reefs and the shortest on the western sides. This trend is less pronounced at more protected reefs (e.g. Wistari and North West) which tend to have uniformly short (15–40 m) grooves on all sides.

The average slope of all grooves in the CBG was 2.5° (Table 3). In total 86% of grooves have a maximum slope of $<5^\circ$ and 93% have a mean slope $<5^\circ$. Sinuosity values showed little variation between or within reefs (Table 3). The mean spacing of grooves at the start of the zone varied between reefs from 17 m (Lady Elliot) to 34 m (Heron). The average distance between grooves increased down the upper reef slope from the start of the zone (mean spacing of 26 m), to the –3 m contour (36 m), to the –10 m contour (56 m).

The majority of grooves in the CBG are oriented to the east (22%), northeasterly grooves account for 20% and southeasterly for 19% (Fig. 4). Only 1% of grooves are oriented westerly. Groove orientation shows a strong spatial autocorrelation (Moran's $I = 0.87$). Grooves are generally oriented in accordance with the side of the reef on which they are located, such that grooves oriented to the east and southeast occur on the east and southeastern sides of reefs with very little variation. At the northernmost tips of the easternmost (exposed) reefs grooves tend to be oriented northeast, rather than north, as shown at One Tree Reef in Fig. 5. By far the longest grooves (mean length of

92 m) are oriented east while the shortest (24 m) are oriented south (Fig. 4). Easterly oriented grooves are also the most closely spaced (mean spacing of 18 m at the start of the zone) while westerly grooves are the furthest apart (mean spacing of 45 m), and have the greatest variability in spacing ($SD = 46$ m) (Fig. 4).

Bifurcation occurs when one groove splits into two (Fig. 3a). This phenomenon has not been studied previously and the mechanism and causes are unknown. A total of 1585 points of bifurcation were identified in this study, equating to 14% of all grooves. Throughout all reefs, bifurcation occurred most commonly in grooves classed as medium exposure (35%), while high and low exposure grooves had lower bifurcation rates (20% and 17% respectively). The geomorphic metrics of bifurcating grooves were similar to the general population of all grooves, except that bifurcating grooves were longer with a median length of 52 m as compared to 31 m for all grooves.

4.2. Relationships between SaG morphometrics and environmental factors

Pertinent results of the Spearman's rank-order correlation analysis are presented in Table 4. Many variables exhibit significant correlations. Correlations follow the same patterns but tend to be stronger in the subset of 11 reefs for which high-resolution bathymetry were available (values in parentheses in Table 4). This suggests that higher data quality yield stronger relationships, thus increasing the confidence in our findings. Most notably, groove length is positively correlated with easterly orientation, width of the upper reef slope, wave exposure, depth and easterly aspect. Groove length is negatively correlated with slope. Exposure is strongly correlated with easterly orientation of grooves and easterly aspect of the reef slope. This is expected given the dominance of east southeasterly trade winds and swells. Exposure is also strongly positively correlated with upper reef slope width and negatively correlated with slope. Mean slope and width of the upper reef slope are also negatively correlated. Easterly aspect of the reef slope and easterly orientation of grooves are strongly positively correlated with each other and with width of the upper reef slope. This shows that reef slopes are wider and less steep on the windward side of reefs in the CBG.

PCA results (Table 5) show how the data transformed across six uncorrelated components with Components 1 and 2 accounting for 59% of total variance in the dataset. Components 3–6 have Eigenvalues less than one and are therefore less important in the description of dataset variability. The dominant variables contributing to variance across Component 1 are exposure (0.92) and groove orientation (0.83) while variance across Component 2 is primarily driven by length (0.95). Slope accounts for the majority of variance in Component 3 and depth dominates Component 4, each of which explain about 12% of the total variance.

4.3. SaG classification

As revealed in the PCA (Table 5), wave exposure, orientation and length were the parameters responsible for the majority of variance in the dataset, while slope and depth also contributed to a lesser extent. The iterative testing process established four classes of SaGs defined by their orientation, length, minimum depth and connection to the reef crest. A Kruskal-Wallis H test confirmed that differences between classes were statistically significant and could not be due to random chance ($p = 0.000$ (all)). The SQL definitions used to define classes are presented in Table 6 with the mean geomorphic and environmental values for each class. The spatial distribution of classes throughout the CBG is shown in Fig. 6.

Extensive ground truthing at the sites shown in Fig. 6, revealed that these classes, created only using variables available from remote sensing, performed very well at distinguishing differences in SaG characteristics, including cross-sectional shape and substrate. The characteristics of each class are described below and depicted in Fig. 7.

Table 3
Relevant geomorphic and environmental metrics for each study reef.

Reef	# grooves	Length (m)			Mean wave exposure class	Mean slope (°)	Mean sinuosity (0–1)	Depth (m MSL)	Reef flat area (km ²)	Mean upper slope width (m)	% of grooves which bifurcate	Mean spacing between adjacent grooves (m)	Grooves/km ² of reef flat	
		Mean	Min	Max										
North ^a	495	72	7	465	74	0.83	High	2.7	0.97	5	0.1	17	2.59	205
Tryon ^a	294	41	4	285	46	0.39	Low	3.6	0.98	5	0.4	20	2.15	110
Broomfield ^a	555	86	4	420	69	0.88	High	2.7	0.98	5	0.4	23	6.38	279
Wilson ^a	980	82	4	118	15	0.17	Low	1.4	0.97	6	0	17	0.91	184
North West	173	28	13	319	60	0.44	Med	3.5	0.98	5	1	22	28.87	156
Wreck ^a	408	96	6	536	90	0.81	High	3.2	0.99	7	0	31	4.07	212
Sykes ^a	738	82	11	654	65	0.72	Med	1.7	0.98	3	0.4	18	6.51	223
Heron ^a	767	34	4	269	30	0.24	Low	3.3	0.98	4	1	13	28.32	187
Wistari ^a	1163	25	3	124	17	0.21	Low	3.5	0.97	3	1	14	23.94	142
Masthead	1214	65	2	402	64	0.75	Med	2.8	0.97	5	1	13	6.85	135
Polnaise	879	32	4	170	22	0.36	Low	0.9	0.97	6	1	14	8.85	177
One Tree ^a	885	45	4	316	37	0.56	Med	1.7	0.98	4	0.3	15	13.30	197
Fitzroy ^a	785	64	4	646	71	0.88	High	2.8	0.98	8	0.1	28	12.56	248
Llewellyn ^a	894	36	4	169	28	0.62	Med	3.3	0.98	4	0	16	12.41	180
Fairfax	329	28	1.5	202	36	0.69	Med	1.9	0.98	6	1.6	23	3.15	129
Lady Musgrave	610	30	5	148	20	0.79	Med	2.8	0.98	4	2.6	20	10.33	155
Lady Elliot	261	43	8	205	32	1.19	High	1.5	0.98	5	0.8	18	1.39	135
Mean	672	52	5	320	46	0.62	Med	2.5	0.98	5	0	19	10.15	180

^a Denotes reefs with high resolution LADS bathymetry which were used to develop the classification.

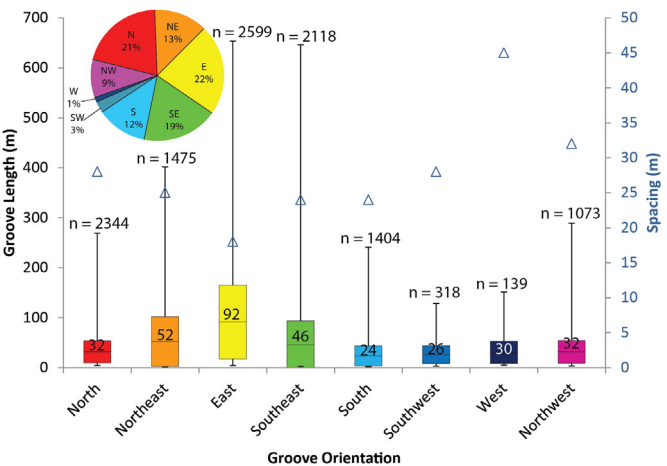


Fig. 4. Groove length (left vertical axis) represented by box plots showing mean length and one standard deviation either side with whiskers representing upper and lower outliers. Grooves are grouped according to orientation. Triangles show mean spacing (right vertical axis) of grooves of each orientation at the start of the SaG zone. The pie chart shows the percentage of grooves orientated in each direction.

Class 1 - Deep and disconnected (DaD), contains grooves deeper than 5.5 m at their shallowest point, which are not connected to the reef crest. They predominantly occur on a 9–20 m terrace and their orientation is different from adjacent spurs on the upper reef slope that are connected to the reef crest (e.g. two satellite images in Fig. 6). DaD spurs generally have relatively low (~50%) coral cover and are dominated by branching or plating *Acropora* and encrusting algae. The features are low relief, ranging in height from ~0.5–1.5 m with a gentle “V” shaped morphology. Spur width varies from ~6–10 m (up to 25 m) and grooves are usually very narrow (0.5–2 m wide) but can reach widths of up to 12 m. The floor of the groove is usually bare reef rock or has a thin veneer of sand and very occasional rubble pieces.

Class 2 - Exposed to wave energy (EWE), contains grooves oriented between northeast (24°) and southeast (158°) and thus are most exposed to wave energy. EWE spurs generally have very high coral cover (~90%) with low morphology, high energy, *Acropora* and *Isopora* dominating the shallow parts of the spur and plating *Acropora* becoming more common on deeper spurs. Spurs range in height from 1 to 2.5 m and 5–23 m in width. Grooves are characterized by a highly channelized “U” shaped morphology, 1–2 m wide, with smooth vertical walls. The floor of the grooves is characterized by large rounded rubble clasts with occasional pockets of coarse sand. In deeper areas further from the reef crest, rippled sand dominates the grooves.

Class 3 - Long and protected (LaP), is oriented opposite to those in Class 2 (southeast 158°, westward to northeast 24°) and have groove lengths > 50 m (which is the mean length of grooves oriented opposite to those in Class 2). LaP spurs generally have high coral cover (80–90%) rich in diversity but dominated by branching and plating *Acropora*, *Isopora* and *Pocillopora*. Spurs range from 1.5–3.5 m in height and from 3 to 12 m in width. Grooves are characterized by highly rugose vertical or overhanging walls with much live coral growth. Groove width varies from 2 to 10 m and grooves are usually floored with rippled carbonate sand, and occasionally, poorly-sorted, moderately small rubble clasts.

Class 4 - Short and protected (SaP), has the same orientation as LaP but are shorter than 50 m (the mean) in length. SaP spurs have the same coral cover and diversity as LaP spurs. They range in height from 1.5–4 m and 4–12 m in width. SaP grooves are generally narrower, ranging from approximately 1–6 m in width, have highly rugose vertical to overhanging walls with live coral growth. Grooves are floored predominantly by poorly sorted, angular rubble, with occasional live corals growing on the rubble and occasional sand patches.

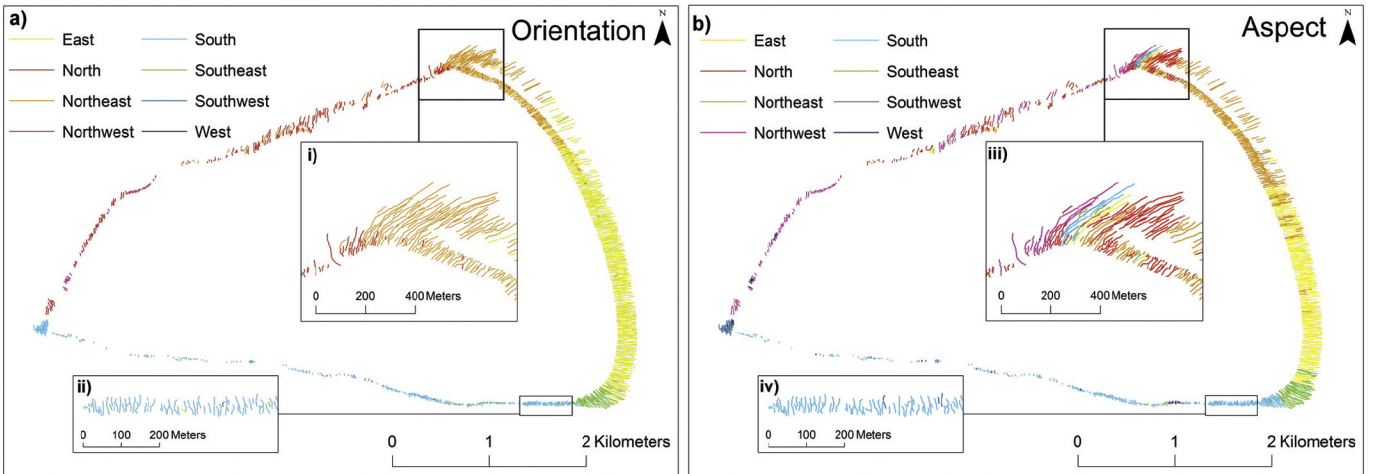


Fig. 5. One Tree Reef showing a) groove orientation and b) aspect of the reef slope. Zoomed areas i) and iii) show how orientation differs to aspect at the northern tip of the reef. Insets ii) and iv) show grooves with the same orientation and aspect on the southern side of the reef.

The majority of grooves (44%) in the CBG fall into Class 2 EWE (Table 6). This class is predominately located on the eastern side of study reefs and is characterized by the widest (mean: 230 m), most gently sloping (mean: 2.3°), upper reef slope (Table 6 and Fig. 6). LaP is the smallest class, only accounting for 5% (604) of all grooves in the CBG. LaP grooves are typically located on the northern to western sides of reefs. DaD grooves are located outside the traditional rim of SaGs and usually occur on an underwater terrace. Where they are located on a terrace, their orientation tends to differ considerably from that of the adjacent grooves on the upper reef slope (e.g. North, Tryon, Wreck, Llewellyn and Lady Musgrave) (satellite images in Fig. 6). SaP grooves are located around the entire western half of reefs and have the narrowest mean upper reef slope (130 m). The highest proportion of groove bifurcation (19%) occurs in Class 3 LaP, though all classes have relatively similar rates.

5. Discussion

To our knowledge, this is the first formally defined, statistically derived morphometric classification of SaGs. The four classes identified in the Capricorn-Bunker Group (CBG), southern Great Barrier Reef, are characterized by substantial differences in cross sectional profile, groove substrate and coral cover which help elucidate the dominant processes in their formation. This classification can be applied elsewhere as it is based on parameters that can be easily measured using remote sensing. Most existing, informal classifications in the literature (summarized in

Table 1) differentiate SaGs based on exposure to wave energy, largely determined by depth. Commonalities between these definitions and the classification presented here include the tendency for shallow/higher energy SaGs to be more closely spaced, and for groove floors to be bare or dominated by rubble in high energy environments and sand in low energy environments. Here we discuss the relationship between SaG morphology and environmental factors; the classification's implications for understanding SaG formation and reef platform evolution in the GBR, and the global applicability of the classification.

5.1. SaG morphology and environmental factors

The morphology of SaG systems is thought to be determined primarily by dominant wave conditions (Storlazzi et al., 2003). By quantifying SaG morphometrics and environmental factors we found statistical evidence to support this assertion. In particular, PCA revealed that relative wave exposure accounts for the most variability in the dataset. Other morphologic factors: depth, slope, aspect and width of the upper reef slope, which are influenced by the morphology of the antecedent Pleistocene basement and subsequent growth of the Holocene reef, also emerged as important but are secondary to wave exposure (Table 5).

The distribution of grooves around each reef was related to the distribution of wave energy, with the majority of grooves occurring on the eastern sides of reefs reflecting the dominance of the east-southeasterly trade wind-driven swell (Fig. 4). Class 2, exposed to wave energy (EWE), was the largest class accounting for 44% of all grooves in the

Table 4

Spearman's rank-order correlation matrix for selected variables. Correlation values in brackets were calculated using only the 11 reefs with high-resolution LADS bathymetry data; other values were calculated using data from all 17 reefs. Significant correlation values at the 0.01 level are marked with two asterisks. One asterisk denotes a significant correlation at the 0.05 level. Particularly strong positive correlations (>0.4) are in bold and strong negative correlations (<-0.4) are underlined.

	Length	Exposure	Mean depth	Mean slope	Aspect (eastness)	Orientation (eastness)	Upper reef slope width
Length							
Exposure	0.274** (0.340**)						
Mean depth	0.177** (0.253**)	0.015 (0.021)					
Mean slope	-0.139** (-0.277**)	-0.123** (-0.282**)	0.333** (0.462**)				
Aspect (eastness)	0.089** (0.353**)	0.266** (0.658**)	0.120** (-0.065**)	-0.379** (-0.316**)			
Orientation (eastness)	0.422** (0.487**)	0.722** (0.729**)	0.046** (0.054**)	-0.116** (-0.343**)	0.247** (0.803**)		
Upper reef slope width	0.403** (0.423**)	0.510** (0.571**)	-0.086** (-0.130**)	-0.183** (-0.410**)	0.182** (0.566**)	0.587** (0.548**)	

Table 5

Varimax rotated principal component matrix of spur and groove metrics. The higher the loading value the greater the contribution of the variable to the component. Dominant contributions (loading > 0.4) are denoted by an asterisk.

Variable	Component					
	1	2	3	4	5	6
Length	0.191	0.954*	-0.064	-0.132	0.032	0.170
Exposure	0.916*	0.083	-0.085	-0.025	0.099	0.160
Mean depth	-0.058	-0.124	-0.161	0.976*	-0.054	0.005
Mean slope	-0.045	-0.062	0.962*	-0.168	-0.173	-0.080
Orientation	0.828*	0.190	0.026	-0.063	0.223	0.236
Upper reef slope width	0.339	0.193	-0.095	0.009	0.109	0.909*
Aspect	0.232	0.032	-0.184	-0.058	0.945*	0.099
Eigenvalue	2.775	1.373	0.849	0.823	0.476	0.412
Percent of variance	39.6	19.610	12.1	11.8	6.8	5.9
Cumulative percent of variance	39.6	59.3	71.4	83.1	89.9	95.8

CBG. Similarly, the distribution of grooves around Bikini Atoll was found to correlate with the distribution of wave power (Munk and Sargent, 1954).

There was a strong positive correlation between length and wave exposure (Table 4). Easterly (exposed to wave energy) grooves in the CBG were the longest and most closely spaced while westerly (protected from wave energy) grooves were significantly shorter and more widely spaced (Fig. 4). For instance, Table 6 shows grooves classified as EWE were more closely spaced than any other class (21 m) while long and protected (LaP) and short and protected (SaP) classes were more widely spaced (32 and 27 m respectively) (Table 6). Deep and disconnected (DaD) grooves had the greatest spacing (42 m) (Table 6). Spacing between all grooves also exhibited a cross-shore trend with spacing increasing with depth from the start of the SaG zone (26 m) to the -3 m contour (35 m) and the -10 m contour (56 m) (Table 3). Similar trends were reported by Storlazzi et al. (2003) in Molokai, Hawaii and by Roberts et al. (1975) in Grand Cayman Island (Fig. 8).

Closer groove spacing in shallower areas where energy is highest suggests that SaGs play a key role in energy dissipation by increasing the surface area of the reef slope as proposed by Munk and Sargent (1954). Physical measurements of waves and currents in SaG zones are lacking in the literature. However, a recent modelling study of SaG hydrodynamics suggested that SaG morphology induces counter-rotating circulation cells which flow onshore over the spurs and offshore through the grooves in shallower water close to the surf zone and the reverse in deeper water (≥ 12 m) further offshore (Rogers et al., 2013). Physical measurements in a SaG system at Palmyra Atoll, a reef exposed to oceanic swell from the North Pacific, supported the

modelling results, showing a persistent 1 cm s^{-1} offshore flow over the spurs and onshore flow over the grooves at depths of 8–11 m (Rogers et al., 2015). However, Rogers et al. (2015) acknowledge that the model results for shallow zones have yet to be verified with field data as instruments were insufficiently shallow, further highlighting the difficulties of collecting data in the shallow, highly dynamic zone. In Grand Cayman Island, a reef exposed to the gentler waves of Caribbean, Roberts et al. (1977) reported that currents in grooves seemed to be tidally dominated. This study also reported data from relatively deep instrument deployments (10 and 22 m). It may be that in shallow areas, and/or during high energy events, SaG hydrodynamics behave differently to those so far measured. Kan (1995) studied sand and coral clast movement under calm and typhoon conditions in SaG zones around Kume Island (Ryukyu, Japan) which is exposed to North Pacific wave energy to a lesser degree than Palmyra Atoll. Kan (1995) found that areas shallower than 12 m experienced extreme clast transport in the typhoon. Direction of sediment transport measured by Kan (1995) during the typhoon was complex with seaward sand flow in approximately 26 m deep grooves, while larger clasts were thrown landward into shallower grooves or up onto the reef flat from grooves shallower than approximately 10 m (see his Fig. 5). The greatest sediment transport and erosion occurred in the widest grooves.

We found the orientation of the grooves was strongly correlated with wave exposure (Table 4) with grooves aligned normal to the direction of incoming refracted waves (Fig. 5). Thus, groove orientation provided an ideal metric to classify SaGs as it faithfully represents wave exposure (Table 4) and can be reliably derived from remotely sensed imagery. SaG orientation in alignment with the direction of wave refraction has also been noted by Roberts (1974) in Grand Cayman Island, Shinn (1963) in the Florida Reef Tract and Weydert (1979) in Madagascar. It has been suggested that grooves were formed by fresh water flows eroding the Pleistocene basement during pre-Holocene sub-aerial exposure (Cloud, 1954; Newell, 1954; and Purdy, 1974). If this were the case, the orientation of grooves would be determined by antecedent topography and they would follow the aspect of the reef slope. Our data shows that, while groove orientation and aspect are often positively correlated (Table 4), the orientation of grooves is not always the same as the aspect of the slope, particularly in high energy EWE SaGs (Fig. 5), thus contradicting the erosion by fresh water flows theory.

The vast majority of grooves (93%) have a mean slope $< 5^\circ$, suggesting that SaG development is limited beyond that slope threshold. Steeper, narrower upper reef slopes were also found to have significantly shorter grooves. For example, grooves in Class 4 SaP were the shortest and had the narrowest mean width of the upper reef slope (130 m) (Table 6). This trend was also noted by Munk and Sargent (1954) at Bikini Atoll, an exposed reef in the North Pacific. SaG zones at other exposed reefs have been reported to occur across gradients of 8.5° and 4° (Palmyra Atoll; Rogers et al., 2015) and 4° (Molokai, Hawaii;

Table 6

Spur and groove classes and their SQL definition. The number of grooves in each class, number of bifurcating grooves and mean groove length, exposure, upper reef slope width, slope, depth and spacing are shown.

Class name	SQL definition	Total	Total bifurcation points	Mean length (m)	Mean exposure	Mean upper slope (m)	Mean width (m)	Mean slope (°)	Mean spacing (m)		
									Start of the SaG zone	-3 m	-10 m
1. Deep and disconnected (DaD)	Minimum depth ≤ 5.5 m AND connected = "No"	1614 (14%)	231 (14% of grooves in that class)	75	0.66 (med)	199	3	11	42	69	45
2. Exposed to wave energy (EWE)	Orientation $\geq 24^\circ$ AND orientation $\leq 158^\circ$	4971 (44%)	677 (14%)	61	0.82 (high)	230	2.3	3	21	26	54
3. Long and protected (LaP)	Length ≥ 50 m AND (orientation $\leq 24^\circ$ OR orientation $\geq 158^\circ$)	604 (5%)	112 (19%)	71	0.19 (low)	152	2.7	4	32	38	58
4. Short and protected (SaP)	Length ≤ 50 m AND (orientation $\leq 24^\circ$ OR orientation $\geq 158^\circ$)	4241 (37%)	430 (10%)	23	0.30 (low)	130	2.7	4	27	34	44

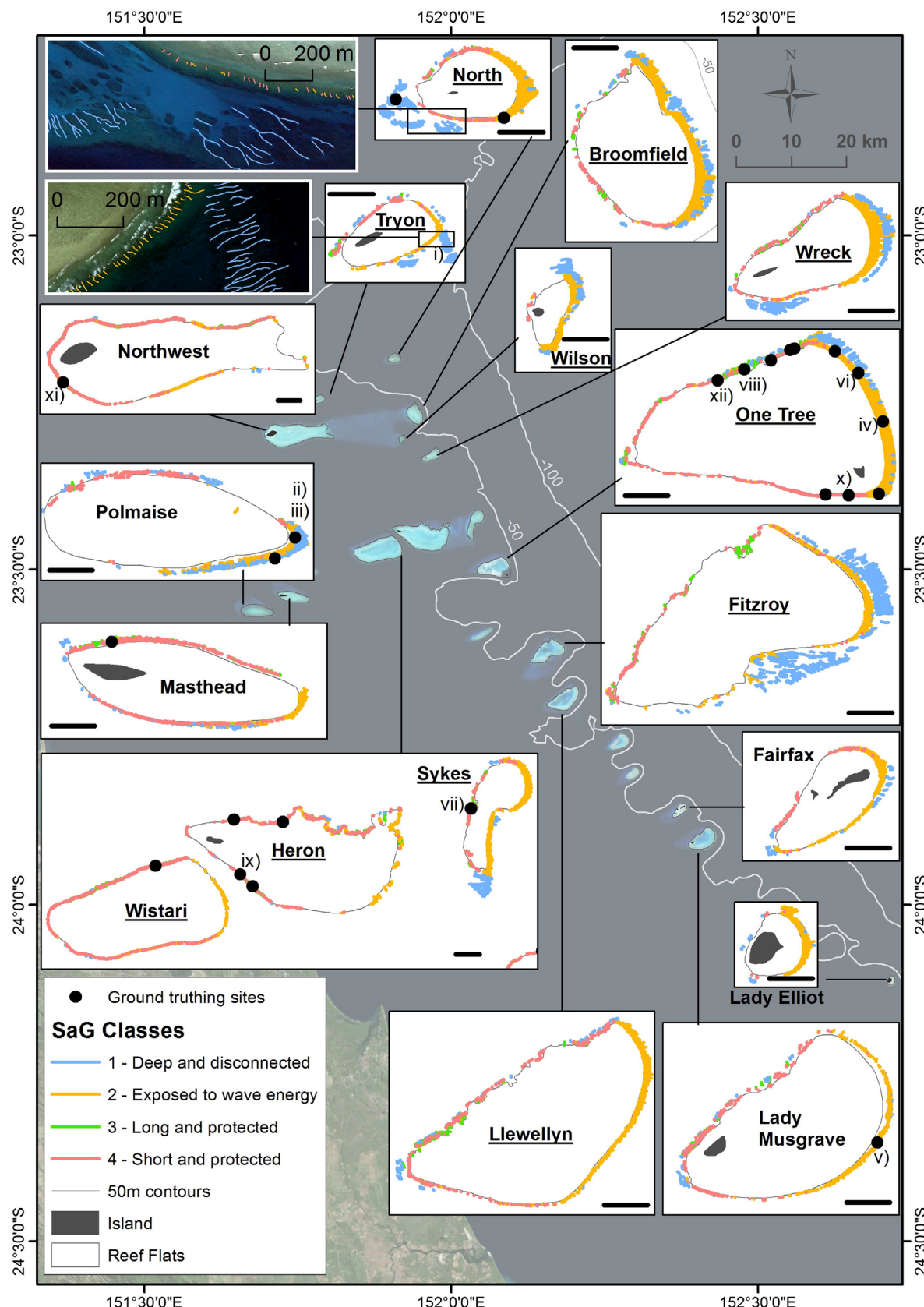


Fig. 6. Spatial distribution of the four SaG classes. Reef insets show black scale bars denoting 1 km. Satellite imagery insets (top left) show the different orientation of DaD grooves on the terrace at North and Tryon Reefs. Black dots show the locations of ground truthing surveys. Labels i) to xii) correspond to pictures in Fig. 7.

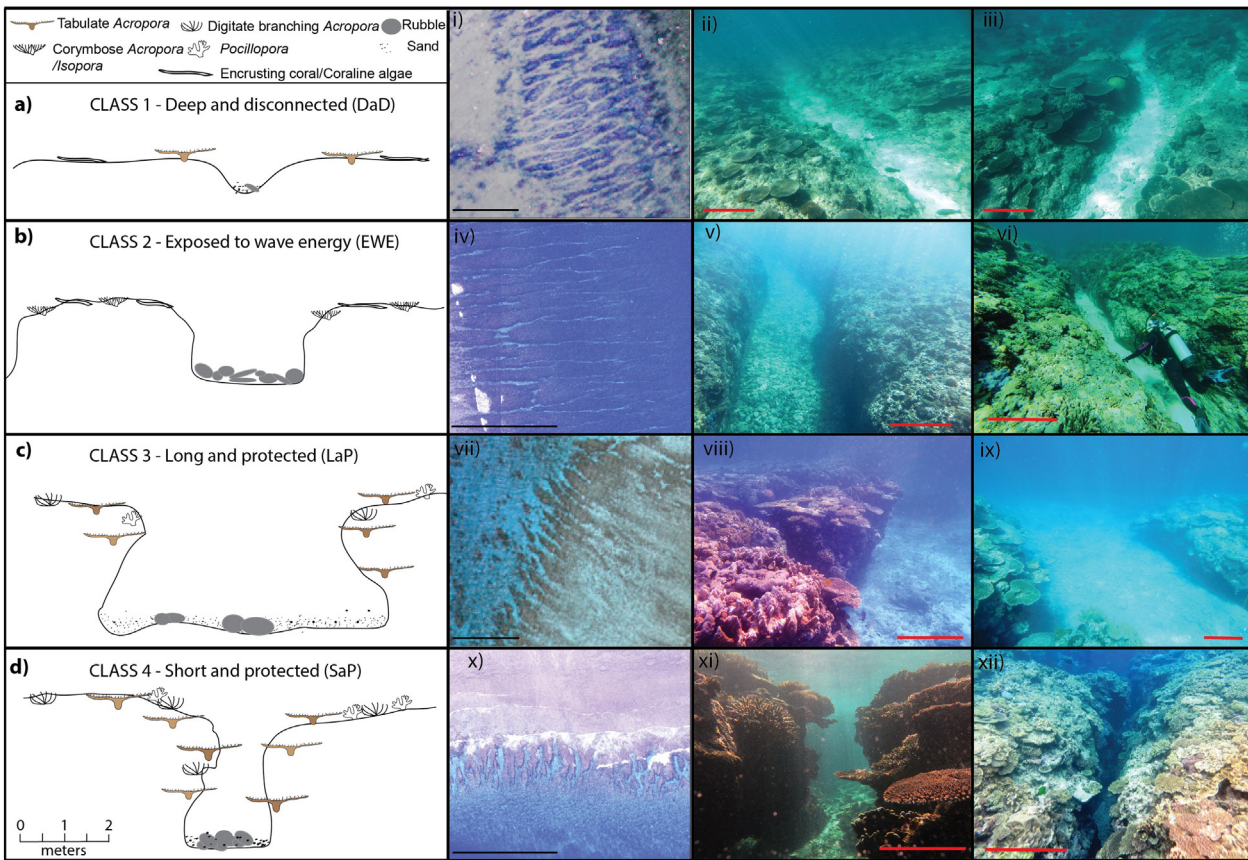


Fig. 7. Characteristic cross-sections of each SaG class (a–d) alongside characteristic plan view images (i, iv, vii, x) and ground truthed images of each class (ii, iii, v, vi, viii, ix, xi, xii). These generic profiles vary in dimensions, but the characteristic shape is the same. Black lines in the plan view images represent scale of 100 m. Red lines in the ground truthed images represent scale of approximately 1 m. **Fig. 6** shows the location of images i to xii. (For interpretation of the references to color in this figure legend, the reader is referred to the web version of this article.)

Rogers et al., 2013). This highlights that gradient and width of the reef slope are determining factors in SaG formation. Thus, while waves seem to be the dominant factor, SaG formation is also dependent on a suitable gradient and width of the upper reef slope.

5.2. Mechanisms for SaG formation and implications from the classification

Coral growth is governed in large part by interactions between light availability, required for photosynthesis (Anthony and Hoegh-Guldberg, 2003), and physical hydrodynamic forces. Hydrodynamic forces can inhibit coral recruitment and cause physical breakage (Madin et al., 2014) but also minimize the deposition of sediment which can be detrimental to coral growth (Fabricius, 2005) and speed calcium carbonate production (Hamylton et al., 2013) by increasing nutrient uptake rates (Hearn et al., 2001). SaGs are an expression of these constructive and destructive interactions. Both erosional (scouring and pruning) and constructional (coral growth and cementation) processes are likely involved in SaG formation to varying degrees depending on the different environmental settings (Shinn, 2011).

5.2.1. Erosion dominated spurs and grooves

We suggest that erosional processes could be the dominant mechanism in the formation of SaGs exposed to wave energy (Class 2 EWE). EWE spurs are lower, ranging in height from 1 to 2.5 m with coral cover of morphologically robust (encrusting or corymbos) species and crustose coralline algae. These spurs display smooth, vertical walls (**Fig. 7iv–vi**). EWE grooves are the most closely spaced and groove substrates are characterized by bare reef rock or rounded clasts of reef debris which transition to sand as depth increases and energy decreases. These characteristics are indicative of powerful flows, scouring and

erosive processes. Storlazzi et al. (2003) found that spur height and coral cover decreased as wave energy increased in Molokai, Hawaii (from 0.5 m spur height at the –5 m contour to 1.1 m at the –15 m contour). They hypothesized that spurs in shallow, high energy areas are constructed by the binding of coral rubble in plentiful supply due to mechanical breaking, by diagenetic cementation, or coralline algae accelerated by constant flushing (Storlazzi et al., 2003). Although this hypothesis has yet to be supported with dating, similar processes may be responsible for the formation of EWE SaGs.

5.2.2. Coral growth dominated spurs and grooves

We suggest that coral growth processes dominate the formation of protected SaGs in class 3 LaP and class 4 SaP (**Fig. 7 vii–ix and x–xii**). These SaGs are characterized by the tallest spurs 1.5–4 m from groove trough to spur crest, with the highest and most diverse coral cover and low exposure to wave energy. The coral covered tops, and overhanging coral covered walls indicate that these spurs are likely growing vertically to sea-level and laterally to eventually coalesce. The presence of considerable sediment in LaP and SaP grooves shows that energy is usually low. Coral rubble, when present, is typically angular and coated with a veneer of sediment, indicating that storms play a role in breaking off and depositing rubble, but energy is too low to constantly re-work the rubble. Roberts et al. (1975) observed that grooves on the deeper (8–22 m), lower energy terrace in Grand Cayman Island were narrower, overhanging and had tunnel structures. They hypothesized the SaG morphology was initiated at lower Holocene sea level and spurs continued to grow vertically and laterally to coalesce as sea-level rose and they were no longer exposed to high wave energy. Conversely, Blanchon and Jones (1997) hypothesized that the same features were formed by coral pruning and sand flushing during episodic hurricanes.

Only three studies have examined SaG development through the radiometric dating of in situ corals (Shinn et al., 1981; Kan et al., 1997a, 1997b). All found spurs were constructional features, not influenced by underlying bedrock. Shinn et al. (1981) found shallow spurs in the Florida Keys, USA, began growing around 6.5 ka when sea level was lower than present in the Caribbean. These spurs were found to grow upwards and landwards as sea-level rose, shaped by coral growth aligned in the direction of dominant hydrodynamic forcing. Kan et al. (1997b) found that spurs at Tonaki Island, Ryukyus (Japan) began growing around 4.45 ka when local sea level was higher than present during the 'Holocene high energy window'. They found the spur started as an offshore patch reef which then grew both landward and seaward facilitating reef flat extension by 400 m since 4.5 ka. As the reef margin prograded seaward the grooves behind became isolated and were infilled by detrital reef sediments. Spurs were also found to extend seaward and landward at Miyako Island in the Ryukyus (Kan et al., 1997a). We suggest LaP and SaP SaGs could be formed predominantly by coral growth in a similar manner. Given that these two classes are often co-located, more research is necessary to understand why LaPs grow longer while SaPs seem to grow wider, narrowing the grooves (Fig. 7).

5.2.3. Relict spurs and grooves

Deep and disconnected SaGs (Class 1 DaD) have the lowest spur height, the greatest mean length, widest mean spacing, lowest coral cover and limited sediment in the grooves (Table 6 and Fig. 7i–iii). These characteristics make them most similar to the highest energy SaGs reported elsewhere (e.g. Molokai; Storlazzi et al., 2003). However, as they occur predominantly on a submerged terrace 9–20 m deep, they are not exposed to high wave energy under present conditions. In addition, they are oriented differently to SaGs on the upper reef slope which are connected to the reef crest (satellite images in Fig. 6).

Other lower terrace SaGs discussed in the literature at Grand Cayman Island have been associated with the energy of unrefracted waves (Roberts, 1974) or episodic extreme energy events (Blanchon and Jones, 1997). The modal wave energy in the CBG is too low (~1.15 m) for unrefracted waves to have any influence on the DaDs at 9–20 m depth. Extreme energy events or strong tidal currents could be related to DaD formation but more research is needed to verify these hypotheses.

Alternatively, these DaD SaGs could represent relict features formed at an early stage in the Holocene transgression as the Pleistocene basement in the region occurs at depths between ~9 and 20 m (Jell and Webb, 2012; Dechnik et al., 2015) (Fig. 1). It appears DaD SaGs are growing on this basement which would have flooded between 11 and 8.5 ka according to the Holocene sea level curve for southeast Australia presented by Sloss et al. (2007). Some authors argue there is evidence of several sea level stillstands during the Holocene transgression on the GBR (e.g. Larcombe et al., 1995). It seems possible that these DaD SaGs could have formed in shallow, higher energy waters during such a stillstand but failed to "keep-up" or "catch-up" to present sea level. However, the latest available information does not support the occurrence of stillstands during the Holocene transgression (Lewis et al., 2013; Lambeck et al., 2014). Another possible explanation for the failure of these SaGs to keep-up or catch-up could be high turbidity. Bostock et al. (2009) showed that mass accumulation rates of siliciclastic sediment were high during early post-glacial sea-level rise in the CBG region. Dechnik et al. (2015) contend that this was, in part, responsible for inhibiting reef growth following the initial flooding of the CBG Pleistocene basement. It is important to note that DaD SaGs were only visited at two sites (North and Polmaise) (Fig. 6). Further study of these DaD SaGs could be critical to understanding how reefs responded to the early transgression and why they were not successful in colonizing the entire Pleistocene basement. Given the relationships identified above between waves and SaG morphology and orientation, these

features could also provide insight into the wave climate during the Holocene transgression.

5.3. Potential role of SaGs in reef evolution in the GBR

Clearly the formation processes dominating different SaGs have important implications for reef platform evolution. The SaG formation processes discussed in Section 5.2 provide mechanisms for seaward reef platform expansion. Traditional models of reef platform evolution in the GBR suggest vertical accretion was followed by lagoonward lateral accretion (e.g. Marshall and Davies, 1982; Marshall and Davies, 1985; Hopley et al., 2007). Recent work by Dechnik et al. (2016) found, contrary to traditional models, protected reefs in the GBR, in particular Heron Reef (CBG), show seaward accretion of the reef platform. Heron Reef is characterized by LaP and SaP SaGs (Fig. 6) which could provide the mechanism for the noted seaward expansion. Conversely, at exposed reefs, in particular One Tree Reef (in the CBG), Dechnik et al. (2016) found lagoonward accretion of the reef platform in line with traditional models. However, no material was dated from seaward of the reef crest in the SaG zone. We revealed a strong, positive correlation between relative wave exposure and width of the upper reef slope, such that eastern areas, with high wave exposure and EWE spurs have a wider, gentler upper reef slope than protected areas (Table 4). This new relationship could suggest that reefs in the CBG may also accrete seaward on the windward side with SaGs providing a potential mechanism.

On Hawaiian reefs it has been reported that high wave energy limits the ability of reefs to fill the available accommodation space (Grossman and Fletcher, 2004). For example, the fringing reef along the southern coast of Molokai is narrower where wave exposure is higher suggesting that reefs are unable to extend seaward due to waves (Storlazzi et al., 2003). Wave energy in the CBG is lower than Hawaii but could still

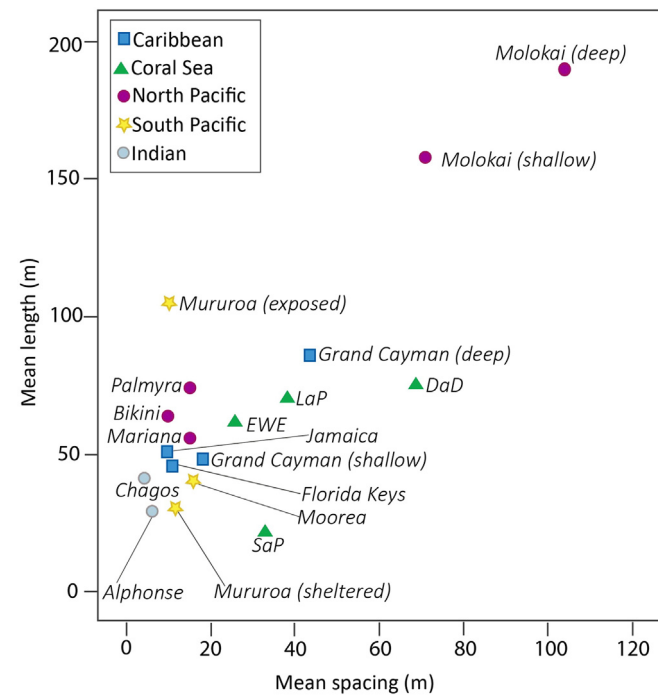


Fig. 8. Comparison of SaGs around the world with respect to length and spacing. The four classes identified in this study are shown as triangles. The other sites in this figure were described in the following published work: Molokai: Storlazzi et al. (2003); Mururoa: Chevalier (1973); Grand Cayman: Roberts (1974); Palmyra: Rogers et al. (2015); Bikini: Munk and Sargent (1954); Chagos: Sheppard (1981); Alphonse: Hamlyton and Spencer (2011); Jamaica: Goreau (1959); Florida Keys: Shinn (1963); Mariana: Cloud (1959). The methodology by which these data were collected is described in Supplementary Table S1.

prohibit the growth mechanisms reported by Shinn et al. (1981) and Kan et al. (1997a) occurring for EWE spurs. In which case, the greater width of the upper reef slope and development of long SaGs on the windward sides of reefs in the CBG may suggest that the antecedent basement on which they grow is larger in extent than present reefs.

Obviously targeted coring and dating of sub-surface facies from all SaG classes are required to confirm or discount the above hypotheses regarding SaG formation mechanisms. Nevertheless, the presence of different SaG classes, with hypothesized differences in formation at a single reef, suggests that Gischler's (2010) division of SaGs into two types, Indo-Pacific and Atlantic characterized by "V" or "U" shaped cross-sectional profiles respectively (Table 1), may be an over simplification. Our findings may call into question the hypothesis that difference in the sea-level history between the two Oceans is the principal driver of morphological differences in SaGs (Gischler, 2010). Without subsurface age data we can only speculate, but as SaGs with different cross-sectional profiles were found throughout an area with the same sea-level history, it would appear that morphological differences are dictated principally by local variations in environmental conditions.

5.4. Global applicability of the classification

The classification presented here performs well in the CBG and is easily applicable elsewhere requiring only remotely sensed imagery, broad scale bathymetry, and a basic understanding of the dominant wave energy regime. Users would need only to digitize grooves and alter the SQL definitions (Table 6) for classes 2, 3 and 4 to reflect the local direction from which dominant wave energy is received. Indeed, digitizing every groove around a reef, as we have in developing this classification, may not be necessary. A random, representative selection of grooves from each sector of the reef, for example the northern, eastern, southern and western sectors, could be digitized and the classification applied to these grooves. Sensitivity testing should be carried out to determine the optimal number of grooves to balance effort and accuracy. Also, continual improvements in spatial and spectral resolutions of remotely sensed images may soon overcome the issues preventing automatic classification of the features as discussed in Section 3.1.1.

Fig. 8 shows a comparison of mean groove length and spacing at reefs globally including the four classes identified in the CBG. This figure shows considerable variability. Indian Ocean SaGs (Alphonse and Chagos) have the shortest, most closely spaced grooves of those examined, while Molokai in the North Pacific (Hawaii) has by far the longest and most widely spaced SaGs. At reefs with more than one data point in Fig. 8, the spacing between grooves is closer for the more exposed/shallow areas (i.e. Molokai shallow; Grand Cayman shallow; Mururoa exposed and CBG Class 2 EWE). However, length does not follow any discernable trend. North and South Pacific reefs with similar energy regimes to Molokai have considerably shorter SaG lengths. This shows that SaG formation processes are complex with many localized environmental factors, besides wave energy, contributing to morphology and evolution.

The SaGs at Molokai are the most morphometrically different to those identified in the CBG. Molokai is exposed to far higher wave energy and is a fringing, rather than a platform, reef. We suggest that at least one additional class would need to be added to our classification for highly exposed reefs. Nevertheless, Fig. 8 shows that the four SaG classes identified in the CBG could be used to describe other SaGs around the world, particularly in moderate to low wave energy settings. Applying this standardized classification elsewhere would help elucidate the complex processes driving SaG formation worldwide.

6. Conclusions

This study quantified metrics at 11,430 grooves across 17 reefs in the Capricorn-Bunker Group, southern GBR, Australia, to reveal important relationships between SaG morphology and environmental factors. In

particular, strong positive correlations between groove length, orientation and wave exposure were identified. These correlations provide quantitative, statistical evidence to support the theory that wave energy is the most important factor controlling SaG distribution and morphology. However, slope was also found to be an important limiting factor, with SaGs less likely to develop in steeply sloping ($>5^\circ$) areas.

Four classes of SaG were identified based on their orientation, length and depth. These morphometric classes, obtained from visual interpretation of satellite imagery, independently distinguish differences in cross-sectional morphology, groove substrate, coral type and percent cover identified in field surveys across 24 sites. These differences provide evidence of the dominant mechanisms of formation at each class. Protected spurs (Class 3 LaP and 4-SaP) appear to be more strongly influenced by coral growth processes while exposed SaGs (Class 2 EWE) appear to be dominated by erosional processes. We also identified for the first time SaGs on the deeper terrace (Class 1 DaD) which are disconnected from the reef crest and may be relict features formed earlier in the Holocene Transgression. These insights, along with our new finding that easterly, exposed upper reef slopes are wider than protected upper reef slopes, have important implication for understanding Holocene reef platform evolution in the region broadly. Further research, including in situ hydrodynamic measurements and collection and dating of closely spaced cores in the SaG zone, is necessary to more fully understand these important processes.

The classes identified here are comparable with SaGs described at other sites though not exhaustive, suggesting the classification could be beneficially applied elsewhere and new classes added. This research revealed considerable geomorphic differences in SaGs across small geographic areas, within the same reef. This indicates that previous SaG classifications based on ocean basin and different relative sea-level histories may oversimplify complex and variable systems driven by localized environmental factors.

Acknowledgments

We are grateful for funding from a Great Barrier Reef Marine Park Authority Science for Management Award (9/1667(2)), Australian Coral Reef Society Danielle Simmons Prize (S.D.), University of Wollongong Return to Work Grant (S.M.H.) and an ARC Future Fellowship (A.V.C., FT100100215). We also thank all staff at One Tree Island and Heron Island Research Station and Russell Graham, Matthew Smith, Rafa Carvalho, Chris Roelfsema, Eva Kovacs, Bevan Yiu, Belinda Dechnik and James Sadler for assistance in the field. We are grateful to Jak McCarroll, Claire Kain and Billy Haworth for useful discussions.

Appendix A. Supplementary data

Supplementary data to this article can be found online at <http://dx.doi.org/10.1016/j.geomorph.2016.04.018>.

References

- Andrefouet, S., 2011. Reef typology. In: Hoyley, D. (Ed.), Encyclopedia of Modern Coral Reefs Structure, Form and Process. Springer, pp. 906–910.
- Anselin, L., 1995. Local indicators of spatial association - LISA. *Geogr. Anal.* 27, 93–115.
- Anselin, L., Syabri, I., Younglin, K., 2006. GeoDa: an introduction to spatial data analysis. *Geogr. Anal.* 38, 5–22.
- Anthony, K.R.N., Hoegh-Guldberg, O., 2003. Variation in coral photosynthesis, respiration and growth characteristics in contrasting light microhabitats: an analogue to plants in forest gaps and understoreys? *Funct. Ecol.* 17 (2), 246–259.
- Battistini, R., Bourrouilh, F., Chevalier, J.-P., Coudray, J., Denizot, M., Faure, G., Fisher, J.-P., Guilcher, A., Harmelin-Vivien, M., Jaubert, J., Laborel, J., Montaggioni, L.F., Masse, J.-P., Mauge, L.-A., Peyrot-Clausade, M., Pichon, M., Plante, R., Plaziat, J.-C., Plessis, Y.B., Richard, G., Salvat, B., Thomassin, B.A., Vasseur, P., Weydert, P., 1975. *Elements de Terminologie Recifale Indopacifique*. *Tethys* 7 (1), 1–111.
- Beaman, R.J., 2010. Project 3DGBR: A High-resolution Depth Model for the Great Barrier Reef and Coral Sea. Marine and Tropical Sciences Research Facility (MTSRF). Cairns, Australia.
- Benhamou, S., 2004. How to reliably estimate the tortuosity of an animal's path: straightness, sinuosity, or fractal dimension? *J. Theor. Biol.* 229 (2), 209–220.
- Blanchon, P., 2011. Geomorphic zonation. In: Hoyley, D. (Ed.), Encyclopedia of Modern Coral ReefsEncyclopedia of Earth Sciences Series. Springer, pp. 469–486.

- Blanchon, P., Jones, B., 1997. Hurricane control on shelf-edge-reef architecture around Grand Cayman. *Sedimentology* 44 (3), 479–506.
- Bostock, H.C., Opdyke, B.N., Gagan, M.K., Fifield, L.K., 2009. Late Quaternary siliciclastic/carbonate sedimentation model for the Capricorn Channel, southern Great Barrier Reef province, Australia. *Mar. Geol.* 257, 107–123.
- Calinski, T., Harabasz, J., 1974. A dendrite method for cluster analysis. *Communications in Statistics - Theory and Methods* 3 (1), 1–27.
- Chevalier, J.-P., 1973. Geomorphology and geology of coral reefs in French Polynesia. In: Jones, O.A., Endean, R. (Eds.), *Biology and Geology of Coral Reefs*, I, *Geology* I. Academic Press, London and New York, pp. 113–141.
- Cloud, P.E.J., 1954. Superficial aspects of modern organic reefs. *Sci. Mon.* 79 (4), 195–208.
- Cloud, P.E.J., 1959. Geology of Saipan, Mariana Islands. US Geol. Surv. Prof. Pap. 280K, 361–445.
- Dechnik, B., Webster, J.M., Davies, P.J., Braga, J.C., Reimer, P., 2015. Holocene “turn-on” and evolution of the Southern Great Barrier Reef: revisiting reef cores from the Capricorn Bunker Group. *Mar. Geol.* 363, 174–190.
- Dechnik, B., Webster, J.M., Webb, G.E., Nothdurft, L.D., Zhao, J.-x., Duce, S., Braga, J.C., Harris, D.L., Vila-Concejo, A., Puotinen, M., 2016. Influence of hydrodynamic energy on Holocene reef flat accretion. *Great Barrier Reef. Quat. Res.* 85 (1), 44–53.
- Demsar, U., Harris, P., Brunsdon, C., Fotheringham, A.S., McLoone, S., 2013. Principal component analysis on spatial data: an overview. *Ann. Assoc. Am. Geogr.* 103 (1), 106–128.
- Drăguț, L., Blaschke, T., 2006. Automated classification of landform elements using object-based image analysis. *Geomorphology* 81 (3–4), 330–344.
- Duce, S., 2009. Towards an ontology for reef island. *Lect. Notes Comput. Sci* 5892, 175–187.
- Duce, S., Janowicz, K., 2010. Microtheories for SDI – accounting for diversity of local conceptualizations at a global level. *Lect. Notes Comput. Sci* 5892, 175–187.
- Duce, S., Vila-Concejo, A., Hamylton, S., Bruce, E., Webster, J.M., 2014. Spur and groove distribution, morphology and relationship to relative wave exposure. *Southern Great Barrier Reef, Australia*, pp. 115–120 (Special Issue 70).
- Ekebom, J., Laihonen, P., Suominen, T., 2003. A GIS-based step-wise procedure for assessing physical exposure in fragmented archipelagos. *Estuar. Coast Shelf S* 57, 887–898.
- Elliott, M., McLusky, D.S., 2002. The need for definitions in understanding estuaries. *Estuar. Coast. Shelf Sci.* 55 (6), 815–827.
- Fabricius, K.E., 2005. Effects of terrestrial runoff on the ecology of corals and coral reefs: review and synthesis. *Mar. Pollut. Bull.* 50 (2), 125–146.
- Gischler, E., 2010. Indo-Pacific and Atlantic spurs and grooves revisited: the possible effects of different Holocene sea-level history, exposure, and reef accretion rate in the shallow fore reef. *Facies* 56 (2), 173–177.
- Goreau, T.F., 1959. The ecology of Jamaican coral reefs I. Species composition and zonation. *Ecology* 40 (1), 67–90.
- Grossman, E.E., Fletcher, C.H., 2004. Holocene reef development where wave energy reduces accommodation space, Kailua Bay, Windward Oahu, Hawaii, USA. *J. Sediment. Res.* 74 (1), 49–63.
- Guilcher, A., 1988. *Coral Reef Geomorphology. Coastal Morphology and Research*. John Wiley and Sons, New York.
- Hamanaka, N., Kan, H., Nakashima, Y., Yokoyama, Y., Okamoto, T., Ohashi, T., Adachi, H., Matsuzaki, H., Hori, N., 2015. Holocene reef-growth dynamics on Kodakara Island (29°N, 129°E) in the Northwest Pacific. *Geomorphology* 243, 27–39.
- Hamylton, S.M., Spencer, T., 2011. Geomorphological modelling of tropical marine landscapes: optical remote sensing, patches and spatial statistics. *Cont. Shelf Res.* 31 (2), S151–S161.
- Hamylton, S., Pescud, A., Leon, J.X., Callaghan, D.P., 2013. A geospatial assessment of the relationship between reef flat community calcium carbonate production and wave energy. *Coral Reefs* 32 (4), 1025–1039.
- Harborne, A.R., Mumby, P.J., Zychaluk, K., Hedley, J., Blackwell, P.G., 2006. Modeling the beta diversity of coral reefs. *Ecology* 87 (11), 2871–2881.
- Harris, D.L., Vila-Concejo, A., 2013. Wave transformation on a coral reef rubble platform. In: Conley, D.C., Masselink, G., Russell, P.E., O'Hare, T.J. (Eds.), 12th International Coastal Symposium. *Journal of Coastal Research*, Plymouth, England, pp. 506–510.
- Hearn, C., Atkinson, M., Falter, J., 2001. A physical derivation of nutrient-uptake rates in coral reefs: effects of roughness and waves. *Coral Reefs* 20 (4), 347–356.
- Hopley, D., 1982. *The Geomorphology of the Great Barrier Reef: Quaternary Development of Coral Reefs*. John Wiley, New York.
- Hopley, D., Smithers, S.G., Parnell, K.E., 2007. *The Geomorphology of the Great Barrier Reef; Development, Diversity and Change*. Cambridge University Press.
- Jain, A.K., 2010. Data clustering: 50 years beyond K-means. *Pattern Recognit. Lett.* 31, 651–666.
- Jell, J.S., Webb, G.E., 2012. Geology of Heron Island and adjacent reefs, Great Barrier Reef, Australia. *Episodes* 35 (1), 110–119.
- Kain, C.L., Gomez, C., Hart, D.E., Chague-Goff, C., Goff, J., 2015. Analysis of environmental controls on tsunami deposit texture. *Mar. Geol.* 368, 1–14.
- Typhoon effects on sediment movement on reef edges and reef slopes. In: Kan, H. (Ed.), *Recent Advances in Marine Science and Technology '94*. PACON International and James Cook University.
- Kan, H., Hori, N., Ichikawa, K., 1997a. Formation of a coral reef-front spur. *Coral Reefs* 16 (1), 3–4.
- Kan, H., Hori, N., Kawana, T., Kaigara, T., Ichikawa, K., 1997b. The evolution of a Holocene fringing reef and island: reefal environmental sequence and sea level change in Tonaki Island, the Central Ryukyus. *Atoll Res. Bull.* 443, 1–20.
- Kuchler, D.A., 1986a. Geomorphological nomenclature: reef cover and zonation on the Great Barrier Reef (ISBN 9780642525215) Great Barrier Reef Marine Park Authority Report, Townsville.
- Kuchler, D.A., 1986b. Reef cover and zonation classification system for use with remotely sensed Great Barrier Reef data (ISBN 9780642525130) Great Barrier Reef Marine Park Authority Report, Townsville.
- Lambeck, K., Rouby, H., Purcell, A., Sun, Y., Cambridge, M., 2014. Sea level and global ice volumes from the Last Glacial Maximum to the Holocene. *Proc. Natl. Acad. Sci. U. S. A.* 111 (43), 15296–15303.
- Larcombe, P., Carter, R.M., Dye, J., Gagan, M.K., Johnson, D.P., 1995. New evidence for episodic post-glacial sea-level rise, central Great Barrier Reef, Australia. *Mar. Geol.* 127 (1–4), 1–44.
- Lewis, S.E., Sloss, C.R., Murray-Wallace, C.V., Woodroffe, C.D., Smithers, S.G., 2013. Post-glacial sea-level changes around the Australian margin: a review. *Quat. Sci. Rev.* 74, 115–138.
- Littler, M.M., Littler, D.S., 2011. *Coralline algae*. In: Hopley, D. (Ed.), *Encyclopedia of Modern Coral Reefs: Structure, Form and Process*. Encyclopedia of Earth Sciences Series. Springer, Netherlands, pp. 20–30.
- Madin, J.S., Baird, A.H., Dornelas, M., Connolly, S.R., 2014. Mechanical vulnerability explains size-dependent mortality of reef corals. *Ecol. Lett.* 17 (8), 1008–1015.
- Marshall, J.D., Davies, P.J., 1982. Internal structure and Holocene evolution of One Tree Reef, southern Great Barrier Reef. *Coral Reefs* 1, 21–28.
- Marshall, J.D., Davies, P.J., 1985. Facies variation and Holocene reef growth in the southern Great Barrier Reef. *Coastal Geomorphology in Australia* 6, 123–133.
- Mathews, E.J., Heap, A.D., Woods, M., 2007. Inter-reef seabed sediments and geomorphology of the Great Barrier Reef, a spatial analysis. *Geoscience Australia Report*.
- Munk, W.H., Sargent, M.C., 1954. Adjustment of Bikini Atoll to ocean waves. U.S. Geological Survey Professional Paper, 260 C, pp. 275–280.
- Newell, N.D., 1954. Reefs and sedimentary processes of Rarotonga. *Atoll Res. Bull.* 36, 1–35.
- Odum, H.T., Odum, E.P., 1955. Trophic structure and productivity of a Windward Coral Reef Community on Eniwetok Atoll. *Ecol. Monogr.* 25 (3), 291–320.
- Pepper, A., Puotinen, M., 2009. GREMO: a GIS-based generic model for estimating relative wave exposure. 18th World IMACS Congress and MODSIM09 International Congress on Modelling and Simulation, pp. 1964–1970.
- Perry, C.T., Murphy, G.N., Kench, P.S., Smithers, S.G., Edinger, E.N., Steneck, R.S., Mumby, P.J., 2013. Caribbean-wide decline in carbonate production threatens coral reef growth. *Nat. Commun.* 4 (1402).
- Purdy, E.G., 1974. Reef configurations: cause and effect. In: Laporte, L.F. (Ed.), *Reefs in Time and Space: Selected Examples from the Recent and Ancient*. Society of Economic Paleontologists and Mineralogists, Oklahoma, USA, pp. 9–76.
- Roberts, H.H., 1974. Variability of reefs with regard to changes in wave power around an island. *Proceedings of the Second International Symposium on Coral Reefs*, Brisbane, 2, pp. 497–512.
- Roberts, H.H., Murray, S.P., Suhayda, J.N., 1975. Physical processes in fringing reef system. *J. Mar. Res.* 33 (2), 233–260.
- Roberts, H.H., Murray, S.P., Suhayda, J.N., 1977. Physical processes in a fore-reef shelf environment. *Proceedings of Third International Coral Reef Symposium*, Miami, pp. 507–515.
- Roelfsema, C.M., Phinn, S.R., 2010. Integrating field data with high spatial resolution multispectral satellite imagery for calibration and validation of coral reef benthic community maps. *J. Appl. Remote. Sens.* 4 (043527), 1–28.
- Rogers, J.S., Monismith, S.G., Feddersen, F., Storlazzi, C.D., 2013. Hydrodynamics of spur and groove formations on a coral reef. *Journal of Geophysical Research: Oceans* 118, 1–15.
- Rogers, J.S., Monismith, S.G., Dunbar, R.B., Kowek, D., 2015. Field observations of wave-driven circulation over spur and groove formations on a coral reef. *Journal of Geophysical Research: Oceans* 120, 145–160.
- Schuenemeyer, J., Drew, L., 2001. *Statistics for Earth and Environmental Scientists*. John Wiley, Hoboken.
- Sheppard, C.R.C., 1981. The groove and spur structures of Chagos atolls and their coral zonation. *Estuar. Coast Shelf S* 12 (5), 549–562.
- Shinn, E.A., 1963. Spur and groove formation on the Florida Reef Tract. *J. Sediment. Petrol.* 33 (2), 291–303.
- Shinn, E.A., 2011. Spurs and grooves. In: Hopley, D. (Ed.), *Encyclopedia of Modern Coral Reefs: Structure, Form and Process*. Encyclopedia of Earth Sciences Series. Springer, Netherlands, pp. 1032–1034.
- Shinn, E.A., Hudson, J.H., Robbin, D.M., Lidz, B., 1981. Spurs and grooves revisited: construction versus erosion Looe Key Reef, Florida. *Proceedings of the Forth International Coral Reef Symposium*, Manila, pp. 475–483.
- Sloss, C.R., Murray-Wallace, C.V., Jones, B.G., 2007. Holocene sea-level change on the southeast coast of Australia: a review. *The Holocene* 17 (7), 999–1014.
- Sneh, A., Friedman, G.M., 1980. Spur and groove patterns on the reefs of the northern gulf of the Red-Sea. *J. Sediment. Petrol.* 50 (3), 981–986.
- Stoddart, D.R., 1978. Descriptive reef terminology. In: Stoddart, D.R., Johannes, R.E. (Eds.), *Coral Reefs: Research Methods*. United Nations Education, Science and Cultural Organisation (UNESCO), Paris, pp. 5–15.
- Storlazzi, C.D., Logan, J.B., Field, M.E., 2003. Quantitative morphology of a fringing reef tract from high-resolution laser bathymetry: Southern Molokai, Hawaii. *Geol. Soc. Am. Bull.* 115 (11), 1344–1355.
- Wallace, C.S.A., Gass, L., 2008. Elevation Derivatives for Mojave Desert Tortoise Habitat Models. *United States Geological Survey Open File Report 2008–1283*, pp. 1–6.
- Webb, G.E., Nothdurft, L.D., Zhao, J.-x., Opdyke, B., Price, G., 2016. Significance of shallow core transects for reef models and sea level curves, Heron Reef, Great Barrier Reef. *Sedimentology* (in press).
- Weydert, P., 1979. Direction de croissance des éperons sur le front d'un récif barrière – L'exemple du Grand Recif de Tuléar (Madagascar). *Mar. Geol.* 30 (3–4), M9–M19.
- Woolsey, E., Bainbridge, S., Kingsford, M., Byrne, M., 2012. Impacts of cyclone Hamish at One Tree Reef: integrating environmental and benthic habitat data. *Mar. Biol.* 159 (4), 793–803.
- Zar, J.H., 1999. *Circular Distributions: Descriptive Statistics*. In: Zar, J.H. (Ed.), *Biostatistical Analysis* Fourth Edition. Prentice Hall, New Jersey, pp. 592–615.